Evaluating Interoperability of Deconfliction Algorithms in UAS Traffic Management

Zeynep Bilgin*†, Matthieu Verdoucq†, Rodolphe Fremond†, Téo Chauvin‡,
Nicolas Durand‡, David Gianazza‡ and Murat Bronz†‡
*Chair of Rotorcraft and Vertical Flight, Technical University of Munich, Munich, Germany
†ENAC Airbus Sopra Steria Drones and UTM Research Chair
‡Fédération ENAC ISAE-SUPAERO ONERA, Université de Toulouse, Toulouse, France
zeynep.bilgin@tum.de
{matthieu.verdoucq, rodolphe.fremond, teo.chauvin, nicolas.durand, david.gianazza, murat.bronz}@enac.fr

***Abstract*—The aim of this study is to investigate how different tactical conflict resolution algorithms perform when operating concurrently within the same airspace at the Very Low Level (VLL). With the rise of Urban Air Mobility (UAM), new Unmanned Aircraft System (UAS) Traffic Management (UTM) must accommodate diverse UTM service providers monitoring several operations. Consequently, tactical conflict resolution may face safety issues due to interoperability limitations in an even more congested airspace. To assess the severity of these limitations, a simulation environment was developed, acting as a UTM service provider capable of supporting and synergizing multiple deconfliction algorithms. Two decentralized tactical deconfliction algorithms, Optimal Reciprocal Collision Avoidance (ORCA) and Potential Guidance Flow (PGFlow), were incorporated into the simulation and tested both individually and together. Through step-wise density scenarios, their performances have been assessed on both safety and cost-efficiency aspects. The results indicate that the simultaneous deployment of our two algorithms offers comparable performances to single method scenarios, demonstrating the feasibility of operating diverse deconfliction tools concurrently in urban airspace.**

***Index Terms*—Advanced Air Mobility, Conflict Resolution, Guidance, Unmanned Aircraft System Traffic Management, Urban Air Mobility**

I. Introduction

Urban Air Mobility (UAM) is a promising solution to ground traffic congestion and CO_2 emissions in densely populated cities. Research conducted in U.S. and Europe region indicates UAM can potentially reduce travel time by up to 55 % in congested areas and if powered by renewable energy, can lower CO_2 emissions by as much as 30 % [1], [2]. This faster and cleaner transportation option also presents a business opportunity, as the European UAM market is projected to reach approximately €4.2 billion by 2030 [3]. Consequently, UAM is gaining growing interest, prompting companies of all sizes to compete in designing the next generation of UTM systems digitalizing the aviation and modernizing the current Air Traffic Management (ATM) [4]. However, urban airspace is inherently limited by physical and regulatory constraints.

This research is funded by ENAC - Airbus - Sopra Steria, Drones and UTM Research Chair.

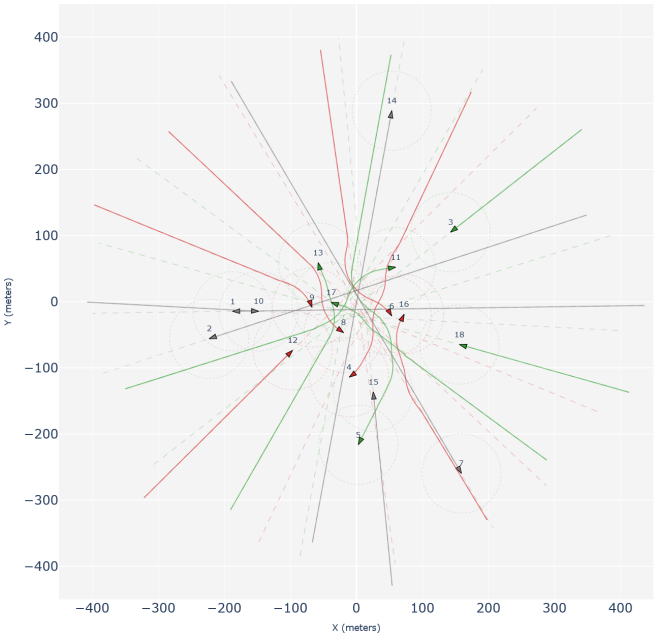

Fig. 1. Multiple deconfliction algorithms, marked with different colored trajectories, operate simulataneously in the same airspace. Dashed lines are the intended flight paths and solid lines are the resultant trajectories after deconfliction efforts. Circles around the vehicles represent the Well-Clear range.

The Very Low Level (VLL) airspace is bounded by terrain, buildings and by restricted zones around airports [5]. Moreover, UAM users are expected to share the same congested airspace with General Aviation (GA), commercial aviation near the airport and their Control Zones (CTZ), and with Unmanned Aircraft Systems (UAS) near vertiports. This high demand for UAM and UAS operations may eventually strain the air traffic regulations and services [6]. In short, as diverse aerial vehicles with varying designs and capabilities enter a previously unregulated and limited urban airspace, conflicts over routing, timing, and separation arise. This requires the development of new ATM systems [5], [7], [8]. Addressing

these challenges requires the development and deployment of conflict management services that ensure safety and efficiency. Tactical conflict resolution, in particular, is essential for managing the interactions among multiple aircraft operating simultaneously in constrained airspace.

Tactical conflict resolution involves a wide range of actors, systems, and processes, each playing a role in the Conflict Detection and Resolution (CD&R) chain [9]. In ATM, CD&R are relying on various tools operating at different time horizons. Medium-Term Conflict Detection (MTCD) tools assist the planning controller by detecting potential conflicts up to 18 minutes ahead. In the short term, Air Traffic Control Officers (ATCOs) are typically alerted by Short-Term Conflict Alert (STCA) systems within minutes of a predicted loss of separation. Collision Avoidance Systems, such as TCAS II, is an airborne and independent system triggered as a last resort, the Resolution Advisories (RA) issued to the pilots must be followed. While UTM may draw on ATM as a model for tactical conflict resolution protocols, research is still ongoing on this advanced service, classified as U4 by EUROCONTROL [10]. Although there are existing standards and recommendations, no binding regulations have been established yet.

CD&R methods for Detect and Avoid (DAA) functions have been comprehensively reviewed and classified in the literature. James K. Kuchar's seminal survey categorised these methods based on detection mechanisms, resolution strategies, and multi-threat scenarios [11]. Building on this foundation, M. Ribeiro provided an updated classification of modern approaches, distinguishing between heuristic, exact, reactive, and explicitly negotiated methods [12].

Among the methods discussed by Kuchar [11] and Ribeiro [12], this work focuses specifically on potential field methods and geometric methods, which can be considered subsets of solution space methods. Potential field methods represent aircraft as high potetial sources, exerting repulsive forces to maintain separation [13], [14]. These methods translate conflicts into vector fields, guiding aircraft away from conflict. Main advantage of potential field methods is their computational efficiency and easy implementation. Geometric methods utilize Velocity Obstacles to determine conflict-free velocity regions [15], [16]. Geometric methods can resolve conflicts by deriving optimal velocites for aircraft that results in minimal trajectory deviations. Notably, Bilimoria [17] analytically computes optimal heading and speed adjustments, ensuring minimal disruption to nominal flight paths. Dowek et al. [18] extended these principles by enabling coordinated maneuvers without explicit intent communication in decentralized conflict management systems.

Integrating such tactical conflict resolution approaches into broader traffic management frameworks is particularly relevant, given the ongoing harmonization efforts by regulatory bodies in the United States and Europe. In the United States, the Federal Aviation Administration (FAA) and the National Aeronautics and Space Administration (NASA) are collaborating on the development of UTM as part of the NextGen initiative [19], which aims to harmonize the VLL within the National Airspace System (NAS). In Europe, EUROCONTROL is a consortium composed of 42 member states (as of 2025) that works closely with the European Union Aviation Safety Agency (EASA) to support the development of a unified European airspace under the Single European Sky (SES) initiative. This includes distinguishing U-space airspace from existing airspace classes, as defined by EU Regulation 2021/664 [10], [20], regulating the provision of U-space services [21], and managing access for manned aviation [22].

For these different ecosystems, the Air Navigation Service Providers (ANSPs) complements the traditional ATM with UTM that needs harmonization. UTM is further challenged by the decentralized architecture of service provisions which does not exclude the possibility of the presence of multiple providers responsible of the same airspace. Those pieces of airspace are orchestrated by single Common Information Service Provider (CISP) that centralizes the information of the operations from the different UTM service providers and keep it available if request by external provider [23]–[25]. Even with a single CISP ensuring all users have the same information, having multiple UTM systems complicates the U-Space management efforts. Managing multiple simultaneous UTM providers remains an active research question and whether the future management will accommodate a multitude of UTM service providers or default to one sole UTM system is still being discussed and needs to be addressed to ensure safe, fair and efficient airspace utilization [25], [26].

This study investigates the concurrent use of two tactical deconfliction algorithms within urban airspace, focusing on their interoperability in their decision-making and global safety performance.

- These algorithms are adapted from guidance for robotics: Potential Guidance Flow (PGFlow) a potential field approach [27] and Optimal Reciprocal Collision Avoidance (ORCA) [28], [29] a geometrical approach, adapted to tactical deconfliction.
- A sandbox simulation environment is developed to evaluate their performances. These scenarios are constructed to simulate conditions where strategic deconfliction has either failed or is absent, placing emphasis on the role of tactical resolution mechanisms with a step-wise density within the urban airspace. In this framework, deconfliction is fully decentralised and may adopt either a single method or a hybrid approach combining both algorithms.
- The evaluation of the scenarios accounts for this multimodal aspect of deconfliction algorithms, which are benchmarked against no-resolution baselines for transparency. The assessment uses safety and cost-efficiency metrics inspired by prior research as well as standards and recommendations for the safety analysis of DAA systems [30].
- Finally, this work aims to explore the viability of integrating multiple tactical deconfliction services, with different deconfliction tools, in shared urban airspace operations.

Future work will extend this study through hardware-in-the-loop testing in a scaled urban environment, incorporating human-in-the-loop air traffic management components to simulate more realistic operational conditions.

The remainder of this paper is organized as follows: Section II describes the simulation setup and system architecture. Section III presents the guidance methods utilized as tactical deconfliction tools. Section IV-A details the measurement metrics and evaluation methodology. Section V discusses the results and findings. Section VI concludes the paper and outlines directions for future research.

II. Simulation Setup

In this study a simulation environment is developed for evaluation of multiple tactical deconfliction strategies. The simulator operates on a single machine, assuming full state observability without any communication delays.
The simulation environment consists in three elements; First, the simulator core that acts as the UTM service provider as detailed in Section II-A. Second, the guidance algorithms that are used in deconfliction as detailed in Section II-B. Finally, the manual controls for the non-cooperative vehicle as detailed in Section II-D. Additionally, the generation of the scenario is detailed in Section II-C.

A. Simulator Core: UTM Service Provider

The simulation framework is mimicking a UTM service provider. The European Union is developing U-space as a unified framework to manage drone traffic safely and efficiently, as well as its integration with ATM. The primary focus of U-Space Service Providers (USSPs) is enabling safe, efficient and secure access to U-Space airspace for numerous drones through digital services [23]. The UTM module in the simulation setup maintains complete knowledge of all vehicles' states, including their positions, velocities, take off and landing locations. Furthermore, the UTM module relays this information to the vehicles and their respective guidance algorithms. These duties are aligned with mandatory U-Space services considered in current EU regulations [20]–[22].

The simulation runs without any communication latency or loss and all vehicle guidance decisions are based on the latest available information. In Fig.2, main components of the simulation setup and their relations are sketched.

B. Guidance Algorithms

The simulator employs guidance algorithms integrated with two different tactical deconfliction algorithms. Each vehicle in the simulation is assigned a guidance method and the guidance algorithms are responsible for the navigation and tactical deconfliction of their assigned vehicles in the simulation. Two algorithms are considered in this study:

- **PGFlow:** Potential Guidance Flow (PGFlow) [27] method requires the vehicle's current position, start and goal locations, and the positions of neighboring vehicles as input. PGFlow computes control actions based solely on positional information, without requiring velocity data.

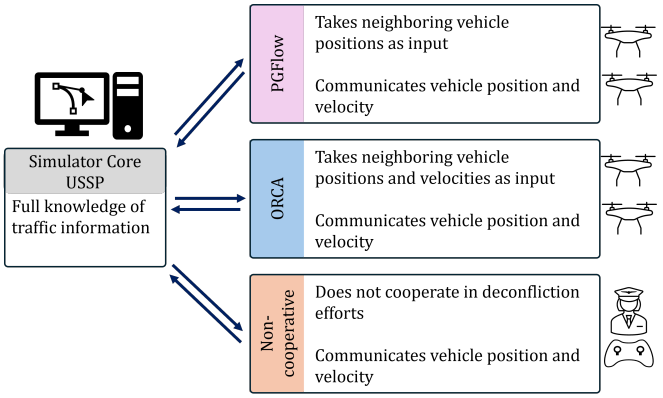

Fig. 2. Simulation Setup. The simulator core has the entire situational traffic awareness and acts as the USSP. Two different deconfliction tools (PGFlow and ORCA) and non-cooperative vehicle(s) are integrated into the simulation environment.

- **ORCA:** Optimal Reciprocal Collision Avoidance (ORCA) [28] algorithm extends the input requirements to include not only the positions but also the velocities of both the subject vehicle and its neighbors.

Both algorithms compute a desired velocity vector to guide the vehicle toward the goal position while also resolving any potential conflicts. This computed vector can be fed directly into the vehicle's flight control system communicated to human operator. In this study the desired velocity vector is used as control input to vehicles directly. Sec.III explains guidance algorithms employed in this study in detail.

C. Scenario Generation

The airspace is modeled as a two dimensional circular area with a specified radius R. For a given number of vehicles, N, start and goal positions are distributed within the circular area favoring the rim rather than the central region.

To generate multiple scenarios with the same number of vehicles, the start and goal positions are perturbed individually. This perturbation is applied locally using a Gaussian distribution centered around the original start and goal locations, rather than uniformly across the entire circle. This method introduces variability between scenarios while maintaining the overall conflict frequency through the randomized initial conditions.

The purpose of this structured scenario generation is to avoid trivial cases with minimal or no conflicts. By concentrating the trajectories toward the center, the likelihood of potential conflicts is increased, providing a more suitable testbed for evaluating tactical deconfliction algorithms. The randomized initialization ensures a wide variety of interaction configurations, promoting the robustness of the evaluation. Upon scenario initialization, all vehicles proceed toward their assigned goals with a preferred speed, randomized between 5m/s and 1m/s under their respective guidance strategies, with tactical deconfliction executed in real-time.

It is important to emphasize that these simulation scenarios should not be interpreted as complete, realistic flight plans. In practice, such densely intersecting trajectories would likely be strategically deconflicted during planning phase and would not be authorized for flight. Instead, these scenarios are intended to represent a localized, emergent situation in which multiple vehicles, despite prior strategic deconfliction efforts, converge into a high conflict area requiring immediate tactical conflict resolution. This approach enables focused evaluation of the tactical deconfliction capabilities of the guidance algorithms.

D. Non-cooperative Vehicle

To simulate more realistic operational environments, a non-cooperative vehicle is introduced. This vehicle can either navigate directly toward its destination without performing any deconfliction maneuvers or can be controlled freely by a human operator. The non-cooperative vehicle's state information (position and velocity) is communicated to the cooperative vehicles through the USSP, enabling cooperative vehicles to perform deconfliction.

This study focuses on analyzing the deconfliction algorithms within a controlled environment by running multiple trials under identical traffic conditions. To maintain replicability across simulations with varying method configurations, the non-cooperative agent feature has not been included in the current simulations. However, this capability will be utilized in future studies involving human-in-the-loop simulations.

III. Guidance Methods

This study employs two different guidance methods for tactical deconfliction. The first method is Potential Guidance Flow (PGFlow) [27] and the second method is Optimal Reciprocal Collision Avoidance (ORCA) [28]. A block diagram for proposed deconfliction algorithms is presented in Fig.3.

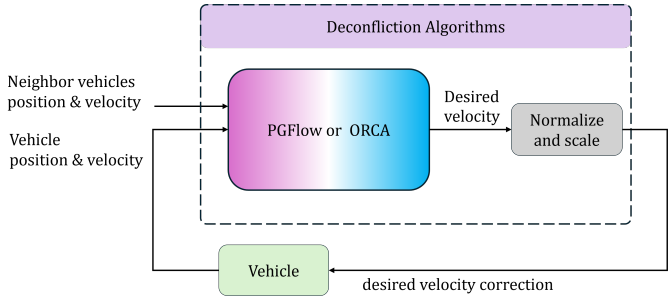

Fig. 3. Block diagram for deconfliction algorithms. The PGFlow guidance algorithm requires vehicle positions as input and ORCA requies both position and velocity information. Both algorithms generate a desired velocity vector to prevent collisions.

In this section both guidance methods are explained in detail; PGFlow in Sec. III-A and ORCA in Sec. III-B.

A. Potential Guidance Flow Method

PGFlow is a vector field based guidance algorithm that generates a guidance vector field using potential flow equations to mimic fluid flow [31]–[33]. The PGFlow algorithm requires the positions of the vehicles in the flight field as input. At each time step, it calculates a guidance velocity that prevents collisions and drives the vehicle towards the goal position. This velocity is then given to the vehicle as the desired velocity. In this study the previously proposed guidance methodology [27] is tailored to fit the requirements and regulations of air traffic control. Following [34], [35] and [27], let $\mathcal{D}$ be a region in $\Re^2$ containing an ideal fluid and $\boldsymbol{P} = (x, y)^T$ be an arbitrary point in $\mathcal{D}$. Let $\boldsymbol{V} = (u, v)^T$ denote the instantaneıus velocity of the fluid at any point. By potential flow theory, the flow velocity at any point $\boldsymbol{P} = (x, y)^T \in \mathcal{D}$ can be calculated by combnining the velocity induced by elementary flow elements in $\mathcal{D}$. The flow velocity calculation in $\Re^2$ is given Eq.1 and Eq.2.

$$u = \sum_{n=1}^{N} \frac{\sigma_n}{2\pi} \frac{x - x_n}{r_n^2} + \frac{\gamma_n}{2\pi} \frac{x - x_n}{r_n^2} + u_\infty \tag{1}$$

$$v = \sum_{n=1}^{N} \frac{\sigma_n}{2\pi} \frac{y - y_n}{r_n^2} + \frac{-\gamma_n}{2\pi} \frac{y - y_n}{r_n^2} + v_\infty \tag{2}$$

Here, u_∞ and v_∞ are components of the free stream velocity. The free stream velocity guides the vehicle towards the goal position and generates smooth trajectories that are easy to follow. The strength of the freestream velocity is determined by the cruise speed of the vehicle. In order to prevent collisions between vehicles, each vehicle in the flight field is modelled as a point source element. Furthermore, to be more synced with current air traffic control regulations, an additional vortex element is assigned to each vehicle. This vortex element forces vehicles to always alter their course to the right in case of a conflict. Here, N is the total number of vehicles in the fleet and source with strength $\sigma_n$is assigned to each vehicle to prevent collisions. γ_n denotes the vortex strength assigned to each vehicle where $\gamma_n = 0.5\sigma_n$ is enforced to ensure vorticity and repulsion is of similar order of magnitude. Position of vehicles are denoted as $\boldsymbol{P}_n = (x_n, y_n)^T$. Reader may refer to [27] for detailed derivation of the PGFlow algorithm.

B. Optimal Reciprocal Collision Avoidance Method

Optimal Reciprocal Collision Avoidance (ORCA) [28] is a geometric collision avoidance algorithm that utilizes velocity obstacles to ensure collision avoidance between moving vehicles.

Fig.4 demonstrates operation of ORCA method for two vehicles A and B. Following [28], [29], let vehicle A and vehicle B have velocities $\boldsymbol{V}_A$ and $\boldsymbol{V}_B$ at $t_0 = 0$ respectively. Let the safe distance to be maintained between vehicles be R; that is, vehicle A should never be in the circle with radius R centered at B. Let $\boldsymbol{V}_r = \boldsymbol{V}_A - \boldsymbol{V}_B$ denote the relative velocity of the vehicle A with respect to vehicle B. If the relative velocity is inside the red cone plotted in Fig.4 loss of separation occurs at some time $t \leq \tau$ [29]. To prevent collision (or loss of separation) both vehicle adjust their velocities so

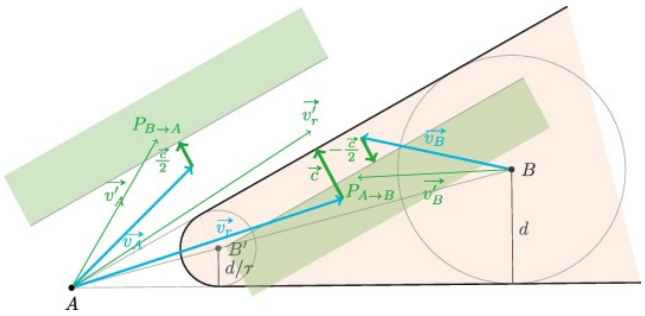

Fig. 4. ORCA velocity obstacle (light red) and admissible velocity domains (in green) for vehicles A and B [29]. If the relative velocity of the vehicle A with respect to vehicle B is in the red cone, collision occurs at time $t \leq \tau$.

that $\boldsymbol{V}_r$ falls outside the velocity obstacle represented by the red cone in Fig.4. The vector $\boldsymbol{c}$ is the adjustment required to move the relative velocity $\boldsymbol{V}_r$ toward the closest boundary of the red cone. Using this vector $\boldsymbol{c}$ collision avoidance domains (green regions in Fig.4) are calculated for each vehicle such that collision avoidance effort is shared equally. At each time step, vehicle A determines its collision free velocity region and chooses a velocity from this region that is nearest to its preferred direction toward its goal. As long as all vehicles apply the same strategy, ORCA enables smooth, coordinated movement and avoids collisions. For more detailed derivation of the method reader can refer to [28], [29].

IV. Experiments

This section begins with the metrics described in Sec.IV-A, followed by the experimental results presented in Sec.IV-B.

A. Metrics

Safety metrics are inspired from the regulated separation layers formalised in ICAO Doc 9863 [36] and adapted for sUAS. Due to the relatively homogeneous performance characteristics of these vehicles, only spatial conditions have been considered in the conflict detection and safety degradation. Two levels of conflict severity are considered in this study:

- Loss of Well-Clear (LoWC): An unsafe separation with relative severity that reqires an immediate resolution. The violation of this layer formalizes a conflict. Set to a horizontal separation below $60m$ in this study.
- Near Mid-Air Collision (NMAC): The highest severity level, indicating that conflict resolution has failed. Set to a horizontal separation below $15m$ in this study.
- Collision: Refers to an actual physical collision between aircraft, defined as a horizontal separation distance of less than $2m$.

Although regulations for conflicts involving exclusively sUAS are still pending, the chosen separation values are consistent with safety measures proposed by the RTCA Special Committees SC-228 and SC-147. These committees focus respectively on UAS performance and Detect-and-Avoid (DAA) systems. The selected thresholds also align with ASTM standards for DAA systems [37], as well as RTCA DO-386 and DO-396, which relate to the development of the ACAS-Xu and sXu systems [38], [39].

While standard separation minima for larger UAS are typically set at 500 ft, several experts have recommended scaling down this threshold for sUAS. This adjustment better reflects the operational characteristics and reduced risk profile of small drones operating in low altitude environments. Specifically, a threshold of 50 ft (i.e. $\approx 15m$) has been cited as an appropriate surrogate for defining NMAC events in such scenarios [40].

The following metrics are computed to assess the safety of the proposed deconfliction algorithms. Eq. 3 reflects the two levels of severity in loss of separation events. While not shown here, the collision rate is computed in a similar manner.

- LoWC Rate: Denoted $\rho(\text{LoWC})$, it represents the average number of LoWC events, N_{LoWC}, occurring per scenario.
- NMAC Rate: Denoted $\rho(\text{NMAC})$, it represents the average number of NMAC events, N_{NMAC}, occurring per scenario.

$$\rho(\text{LoWC}) = \frac{N_{\text{LoWC}}}{N_{\text{scenario}}}, \qquad \rho(\text{NMAC}) = \frac{N_{\text{NMAC}}}{N_{\text{scenario}}} \tag{3}$$

Eq.4 introduces the conflict escalation which gives the probability of escalating from a given LoWC, to a NMAC.

$$\mathbb{P}(\text{NMAC} \mid \text{LoWC}) = \frac{\rho(\text{NMAC})}{\rho(\text{LoWC})} \tag{4}$$

The Risk Ratio, introduced in Eq. 5, is a standard metric used to quantify the safety benefits of a conflict resolution method. It compares the likelihood of a NMAC occurring after a LoWC, with and without the use of a conflict resolution tool, under similar initial conditions.

$$\text{Risk Ratio} = \frac{\rho(\text{NMAC})_{\text{Resolution}}}{\rho(\text{NMAC})_{\text{Direct}}} \tag{5}$$

While derived from the previous equations, Eq. 6 provides a more comprehensive representation of the benefits of conflict resolution through the deconfliction success rate. Note that the similarity between the metrics arises from the assumption that a conflict is considered to occur whenever a LoWC is detected. In practice, however, conflict detection for UTM may involve a temporal component; here, we focus solely on conflict resolution.

$$\text{Deconfliction } (\%) = 100 \times \frac{N_{\text{LoWC}} - N_{\text{NMAC}}}{N_{\text{LoWC}}} \tag{6}$$

In the absence of a resolution method, deconfliction success refers to cases where a LoWC does not result in a NMAC, potentially indicating a false alert.

The scenario's complexity is reflected in the frequency of LoWC events when no resolutions are provided, equal to $\rho(\text{LoWC})_{\text{No Resolution}}$. While this value alone is not directly exploitable, it becomes meaningful when compared across different scenarios, as it illustrates how frequently conflicts occur and require mitigation.

Operational efficiency is evaluated based on deviations from the planned direct routes using the path efficiency, denoted η_{path} and defined in Eq.7. This metric represents the ratio of the distance flown with resolution to that without resolution, serving as an approximation of the average delay when neglecting small speed variations.

$$\eta_{\text{path}} = \frac{d_{\text{direct}}}{d_{\text{resolution}}}, \text{ Delay } (\%) \approx 100 \times (1 - \eta_{\text{path}}) \quad (7)$$

Here, d_{direct} denotes the straight-line distance between the entry and exit points of the conflict scenario sector, as illustrated in Fig.5, assuming no conflicts occurrence. In contrast, $d_{\text{resolution}}$ represents the actual distance travelled when deconfliction algorithms are applied.

B. Results

This section presents the results obtained from batch simulations designed to evaluate the concurrent performance of two conflict resolution approaches. Three case studies with increasing complexity are examined, involving 4 in Sec.IV-B1, 8 in Sec.IV-B2, and 16 vehicles in Sec.IV-B3.

For each case, a Monte Carlo simulation comprising 1,000 trials was conducted, testing various combinations of conflict resolution approaches: ORCA, PGFlow, a mixed approach with equal proportions of the two methods, and a baseline benchmark using no tactical conflict resolution (i.e., Direct).

1) 4 Vehicle Scenario : Fig. 5a presents a snapshot of a Monte Carlo simulation involving 4 vehicles in a hybrid conflict resolution configuration: 2 vehicles use ORCA, and the other 2 use PGFlow. The vehicles largely maintain their intended trajectories, making only slight heading adjustments to avoid NMACs, thereby preserving visual path efficiency. All four operate within a circular area of 0.1465 NM^2, corresponding to a traffic density of 27.3 vehicles per NM^2.

Table I summarises the safety and efficiency performance of the algorithms used individually and in combination (i.e. hybrid configuration) in this scenario.

TABLE I: Conflict resolution performance comparison with 4 vehicles.

Metric	Direct	ORCA	PGFlow	Hybrid
LoWC rate	7.15×10^{-4}	6.57×10^{-4}	2.84×10^{-4}	4.58×10^{-4}
Conflict Escalation (%)	26.73*	3.23	8.71	8.90
NMAC rate	1.91×10^{-4}	2.13×10^{-5}	2.48×10^{-5}	4.08×10^{-5}
Risk ratio	1.00	0.11	0.13	0.21
Deconfliction_success (%)	73.27**	96.77	91.29	91.10
η_{path} (%)	100.00	99.96	94.60	98.28

* *Proportion of LoWC that naturally lead to NMACs. (True Alerts)*
** *Proportion of LoWC that actually do not lead to NMACs. (False Alerts)*

In this experiment, ORCA demonstrates the strongest safety performance, with only one NMAC every 12 trials on average and just 4 collisions over 1,000 simulations. It achieves a high deconfliction success rate of 96.77% and keeps the average number of LoWC events (2.63 per trial) close to the non-resolution baseline (Direct, 2.862 per trial), indicating that

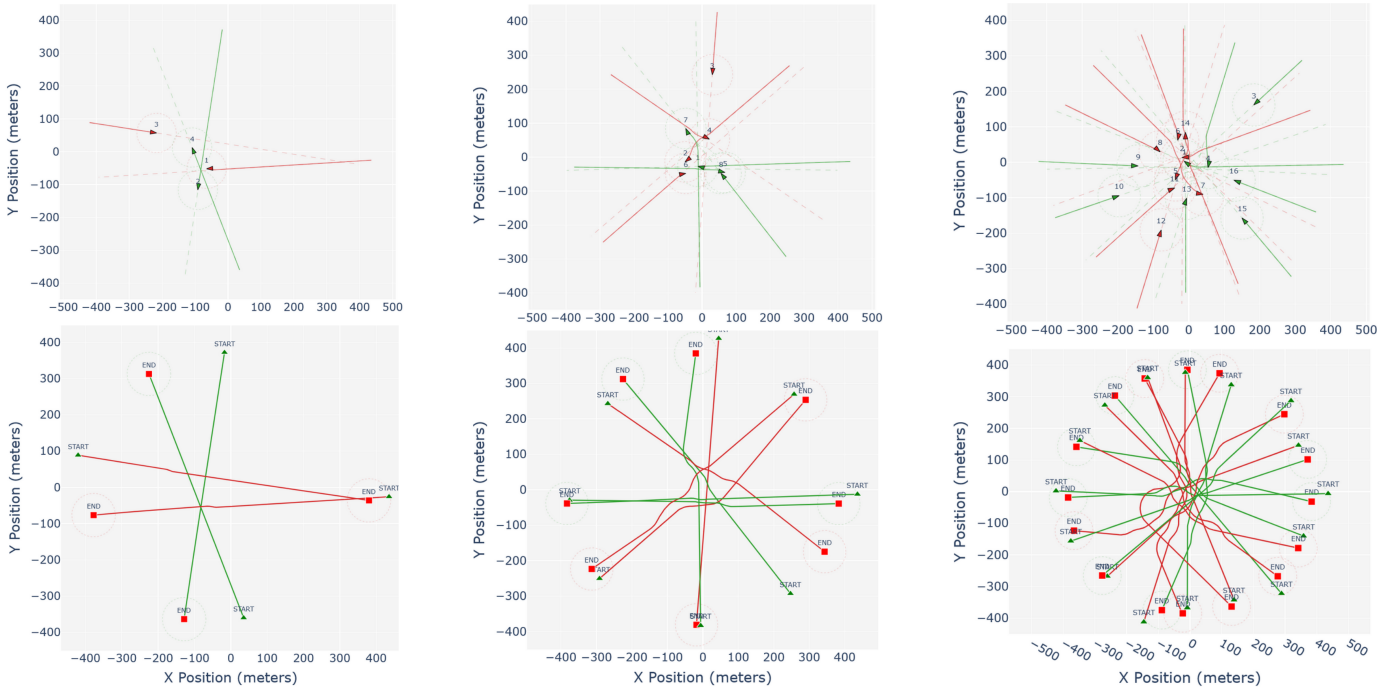

(a) 4 vehicles (b) 8 vehicles (c) 16 vehicles

Fig. 5. Hybrid tactical conflict resolution scenarios using both ORCA (green) and PGFlow (red) in equal proportion across three stepwise traffic density cases. The top figures show scenario snapshots during in-progress conflict resolution with visible LoWC ranges, while the bottom figures present the resultant trajectories at the end of each scenario.

most LoWCs are safely resolved before escalating to NMACs. PGFlow has a higher escalation rate of 8.71% but is more effective at suppressing LoWC events, averaging only 1.14 per trial. This reduced exposure results in a low NMAC rate to up to one per 10 trials, having a risk ratio comparable to ORCA despite more frequent escalations. The hybrid configuration demonstrates intermediate results. It shows a moderate LoWC rate (1.83 per trial) but a higher escalation rate (8.90%) than ORCA, leading to a risk ratio of 0.21. This suggests that while combining both algorithms offers a balance, it is less robust than using either algorithm independently in this scenario.

Table I is complemented by Fig. 6, which presents the percentile distribution of LoWC severity. This plot illustrates how deeply intruders penetrate from the LoWC threshold toward the NMAC threshold , and how well each algorithm constrains these violations.

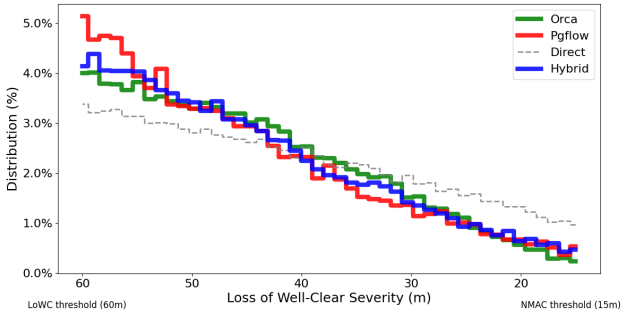

Fig. 6. LoWC severity for 4 vehicle scenario.

We observe that all three resolution strategies (i.e., ORCA, PGFlow, and Hybrid) significantly reduce the number of deep penetrations compared to the Direct baseline. Notably, most separation losses are constrained above 40 m, and very few fall below 30 m. The hybrid approach mirrors ORCA's distribution near the LoWC threshold, while exhibiting similarities to PGFlow closer to the NMAC threshold, indicating complementary behavior in terms of severity control but not competitive with the two algorithms when solely used for this scenario.

2) 8 Vehicle Scenario : Fig.5b presents a snapshot of a Monte Carlo simulation involving 8 vehicles operating in a hybrid conflict resolution configuration with a traffic density of 54.6 vehicles per NM^2. In this setup, 4 vehicles use ORCA while the other 4 rely on PGFlow. Compared to the 4-vehicle case in Fig.5a, the interaction environment is noticeably denser, with more frequent path overlaps and intersections.

The trajectories appear more evasive, especially for vehicles governed by PGFlow, as visual evidence of more aggressive deconfliction maneuvers. This observation is supported by Table II, where the path efficiency for PGFlow drops to 88.88%. In contrast, ORCA retains relatively high efficiency at 97.76%, suggesting more conservative and resilient maneuvering under increased traffic complexity.

Interestingly, the results reveal a shift and nuances in safety performance, with PGFlow outperforming ORCA in terms of

TABLE II: Performance metrics comparison across scenarios with 8 vehicles.

Metric	Direct	ORCA	PGFlow	Hybrid
LoWC rate	2.25×10^{-3}	1.41×10^{-3}	5.28×10^{-4}	1.10×10^{-3}
Conflict Escalation (%)	28.32*	7.21	12.98	13.55
NMAC rate	6.37×10^{-4}	1.02×10^{-4}	6.85×10^{-5}	1.49×10^{-4}
Risk ratio	1.00	0.16	0.11	0.23
Deconfliction_success (%)	71.68**	92.79	87.02	86.44
η_{path} (%)	100.00	97.76	88.88	94.12

* *Proportion of LoWC that naturally lead to NMACs. (True Alerts)*
** *Proportion of LoWC that actually do not lead to NMACs. (False Alerts)*

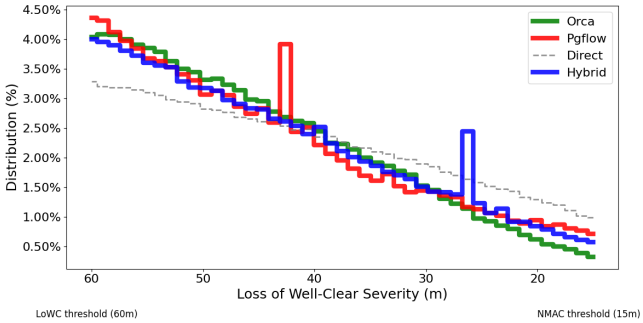

Fig. 7. Severity of Loss of Well Clear for 8 vehicle scenario.

risk ratio (0.11 vs. 0.16). On average, PGFlow results in 0.548 NMACs per trial and one collision every 6 trials, compared to 0.816 NMAC and 1 collision every 9 trials for ORCA. This improved safety is mainly due to PGFlow's lower LoWC rate, indicating better resilience at earlier stages of conflict.

However, ORCA maintains an advantage in limiting conflict escalation, with only 7.21% of LoWC cases progressing to NMACs, compared to 12.98% for PGFlow. Fig.7 supports this analysis by illustrating the severity distribution of LoWC. Both algorithms demonstrate similar capabilities in reducing deep penetrations toward the NMAC threshold. ORCA, in particular, constrains most encounters above 30 metres with stronger containment of conflict severity despite higher LoWC exposure.

The hybrid configuration remains consistent with its 4-vehicle performance, though impacted by the increased scenario complexity. It produces an average of more than 1 NMAC per trial and 2 collisions every 7 trials, leading to a risk ratio of 0.23. While the hybrid still performs better than the direct case, it does not match the individual performance of PGFlow or ORCA under high-density conditions.

3) 16 Vehicle Scenario : Fig.5c presents a snapshot of a Monte Carlo simulation involving 16 vehicles operating under a hybrid conflict resolution configuration, where 8 vehicles use ORCA and the remaining 8 use PGFlow. This scenario represents the densest environment, with a traffic density of 109.2 vehicles per NM^2. As a result, the trajectories show more pronounced deviations and sharper maneuvers with complex interactions triggered by the resolution algorithms.

Despite the increased complexity, the performances shown in Table III reveal improvements over the 8-vehicle scenario discussed in Sec.IV-B2. PGFlow continues to outperform

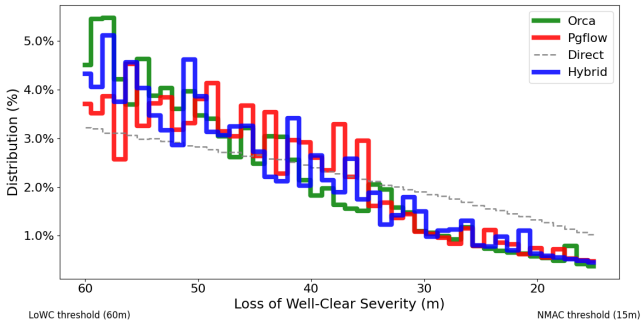

Fig. 8. Severity of Loss of Well Clear for 16 vehicle scenario.

ORCA in terms of safety, achieving the lowest risk ratio of 0.09 compared to 0.13 for ORCA. Additionally, PGFlow demonstrates a reduced conflict escalation rate (8.61%) compared to ORCA (17.85%) highlighting better control of conflict evolution under dense traffic conditions.

TABLE III: Performance metrics comparison across 16 vehicle scenarios.

Metric	Direct	ORCA	PGFlow	Hybrid
LoWC rate	5.40×10^{-3}	2.58×10^{-3}	9.20×10^{-4}	2.04×10^{-3}
Conflict Escalation (%)	32.62*	8.61	17.85	13.93
NMAC rate	1.76×10^{-3}	2.22×10^{-4}	1.64×10^{-4}	2.85×10^{-4}
Risk ratio	1.00	0.13	0.09	0.16
Deconfliction_success (%)	67.38**	91.39	82.15	86.07
η_{path} (%)	100.00	92.61	75.33	86.70

* *Proportion of LoWC that naturally lead to NMACs. (True Alerts)*
** *Proportion of LoWC that actually do not lead to NMACs. (False Alerts)*

As visible also for the distribution of the two previous scenarios, Fig. 8 also shows the behavior of the algorithms to constraint the separation over 40meters and significant safety benefits with poor distribution of intruders below 30 meters apart.

Importantly, the performance of the hybrid configuration has slightly decreases but not drastically, which follows a certain equilibrium between ORCA and PGFlow respective performances.

V. Discussion

This section begins with a comparative analysis of the experimental results in Sec.V-A, followed by a discussion of the key challenges met during the research in Sec.V-B. Finally, Sec.V-C outlines potential directions for future work.

A. Comparative Analysis

The three conflict resolution strategies (i.e., ORCA, PGFlow, and Hybrid) were evaluated through three case studies of increasing complexity. From a safety perspective, PGFlow outperformed the others in the 8 and 16 vehicles' scenarios, achieving the lowest risk ratios and NMAC counts. In contrast, ORCA performed best in the simplest (i.e., 4 vehicles) scenario, demonstrating strong mitigation of NMACs from existing LoWC events, supported by its low conflict escalation rate.

The hybrid approach, combining ORCA and PGFlow in equal proportion, delivered comparatively weaker performance, especially in lower density cases. However, its performance in the 16 vehicles' scenario was close to the single strategy approaches, suggesting that hybridisation remains a viable option in dense environments.

A key observation is that ORCA and PGFlow differ significantly in conflict handling philosophy. ORCA is conservative, prioritizing minimal deviation and reacting to conflicts by subtle corrections, resulting in higher LoWC rates but strong containment of NMACs. PGFlow, on the other hand, is more proactive and evasive, reducing the number of LoWC events by making earlier and more pronounced maneuvers, often avoiding the central hotspot of the scenario altogether.

Finally, across all algorithms, we observe a degree of resilience to increasing conflict density when using the direct (i.e., non-resolution) scenario as a benchmark. Specifically, the number of LoWC events rises from 2.862 (4 vehicles) to 17.988 (8 vehicles), and then to 86.442 (16 vehicles). Despite this increase, safety does not degrade proportionally when applying our conflict resolution strategies, reflected in significantly lower risk ratios and demonstrating their capabilities in mitigating conflicts under higher traffic densities.

B. Challenges

Despite their different behavioral logics, the combination of ORCA and PGFlow shows potential for complementarity, though current results indicate limitations in interoperability, possibly due to the lack of coordination between strategies that do not communicate intent.

The primary contributions of this work include the development of the described simulation environment and the comprehensive evaluation of simultaneous deployment of multiple deconfliction algorithms. The results support the concept of mixed algorithm airspace management. Given the complexity and diversity of urban air mobility operations, understanding the feasibility and integration methods for multiple tactical deconfliction services is a critical research direction. This study represents a valuable initial step toward addressing these challenges.

C. Future Work

Significant effort has been devoted to optimizing the parameters of both ORCA and PGFlow to extract their best individual performance in use case scenarios involving small UAS and narrow separation margins. However, achieving effective interoperability between these two algorithms still requires further investigation, particularly to identify potential synergies and avoid behavioral conflicts.

Ongoing work focuses on adapting and testing these algorithms for larger-scale demonstrations, with increased operational realism. In particular, we are deploying them into a mixed-reality environment, where a real vehicle interacts with synthetic intruders. This setup enables the evaluation of algorithmic performance under real-world dynamics, sensor

noise, and environmental disturbances, while ensuring safety through controlled virtual threats.

In parallel, new conflict resolution strategies are being introduced, including a Reinforcement Learning-based approach and a prototype inspired by the ACAS-sXu framework. These additions aim to enrich the comparative landscape by integrating more mature, standard-aligned solutions and enabling analysis of intent communication and decision-making in heterogeneous environments.

Finally, a human-centric layer will be explored on top of the mixed-reality setup to assess how UTM service providers can efficiently leverage these algorithms. This includes evaluating human-machine teaming, workload reduction, and trust in automation—critical elements in addition to the interoperability between centralized and decentralized conflict resolutions.

VI. Conclusion

This study investigated the concurrent deployment of multiple tactical conflict resolution approaches in urban airspace, specifically focusing on the interoperability and collective performance of Potential Guidance Flow (PGFlow) and Optimal Reciprocal Collision Avoidance (ORCA) algorithms. Extensive simulations were conducted across various small scale scenarios featuring step-wise densities, with 4, 8, and 16 vehicles evaluated under three configurations: exclusively ORCA, exclusively PGFlow, and a hybrid setup combining both methods.

These scenarios have been duplicated without resolution to benchmark the performance of the different approaches. Additionally, a flexible and extensible simulation framework was developed to accommodate the simulation environment and the decentralized algorithms. Our sandbox supports batch simulations in order to stress-test the different conflict resolution algorithms based on their safety and operational efficiency.

Simulation results highlight distinct performance characteristics of the two methods. First, PGFlow consistently demonstrated superior conflict resolution safety performance across most of the scenarios in minimizing LoWC while the path efficiency is discutable. Secondly, ORCA shows a competitive safety performance when considering LoWC that needs to be mitigated in addition to get a great efficiency.

The research results highlight promising opportunities to improve the interoperability of conflict resolution algorithms through mixed-reality deployments, offering precious insights into how conflict resolution strategies at the tactical level might operate in future urban airspace environments.

References

[1] A. Straubinger, R. Rothfeld, M. Shamiyeh, K.-D. Büchter, J. Kaiser, and K. O. Plötner, "An overview of current research and developments in urban air mobility–setting the scene for uam introduction," *Journal of Air Transport Management*, vol. 87, p. 101852, 2020.

[2] L. Moua, J. Roa, Y. Xie, and D. Maxwell, "Critical review of advancements and challenges of all-electric aviation," in *International Conference on Transportation and Development 2020*. American Society of Civil Engineers Reston, VA, 2020, pp. 48–59.

[3] EASA, "Study on the societal acceptance of urban air mobility in europe," in *European Union Aviation Safety Agency*, 2021.

[4] RolandBerger, "How air taxis and freight drones are revolutionizing the future of transportation." Retrieved 12 November, 2020, from. https://www.rolandberger.com/en/Insights/Global-Topics/Urban-Air-Mobility/, 2022.

[5] International Transport Forum (ITF), "Ready for take-off? integrating drones into the transport system," 2021. [Online]. Available: https://www.itf-oecd.org/sites/default/files/docs/take-off-integrating-drones-transport-system.pdf

[6] FAA, "Urban air mobility concept of operations," Version 2.0, U.S. Department of Transportation, 2020. [Online]. Available: https://www.faa.gov/sites/faa.gov/files/Urban%20Air%20Mobility%20(UAM)%20Concept%20of%20Operations%202.0_1.pdf

[7] R. Hansman and P. Vascik, "Constraint identification in on-demand mobility for aviation through an exploratory case study of los angeles," May 2018.

[8] G. Riccardi, L. Brucculeri, E. Fornaciari, M. D'Onofrio, A. Zilli, D. Leanza, G. Ferrara, M. Molinario, G. Esposito, and A. Favier, "CORUS-XUAM: Tackling urban air mobility airspace integration challenges," in *Proceedings of the 34th Congress of the International Council of the Aeronautical Sciences (ICAS 2024)*. International Council of the Aeronautical Sciences, 2024. [Online]. Available: https://www.icas.org/icas_archive/icas2024/data/papers/icas2024_0347_paper.pdf

[9] M. Johnson and J. Larrow, "UAS traffic management conflict management model," *NASA*, 2020.

[10] SESAR JU, "U-Space Blueprint," 2019, accessed online: 2024-12-19.

[11] J. Kuchar, L. Yang, and L. Yang, "Survey of conflict detection and resolution modeling methods," *AIAA, Guidance, Navigation, and Control Conference*, 1997.

[12] M. Ribeiro, J. Ellerbroek, and J. Hoekstra, "Review of Conflict Resolution Methods for Manned and Unmanned Aviation," *Aerospace*, vol. 7, 2020.

[13] M. Eby, "A self-organizational approach for resolving air traffic conflicts," *Lincoln Laboratory Journal*, vol. 7, no. 2, 1994.

[14] J. Hoekstra, R. van Gent, and R. Ruigrok, "Designing for safety: The 'free flight' air traffic management concept," *Reliability Engineering & System Safety*, vol. 75, pp. 215–232, 2002.

[15] Y. I. Jenie, E. J. van Kampen, C. C. de Visser, J. Ellerbroek, and J. M. Hoekstra, "Selective velocity obstacle method for deconflicting maneuvers applied to unmanned aerial vehicles," *Journal of Guidance, Control, and Dynamics*, vol. 38, no. 6, pp. 1140–1146, 2015.

[16] S. V. Dam, M. Mulder, and R. Paassen, "The use of intent information in an airborne self-separation assistance display design," in *AIAA Guidance, Navigation, and Control Conference*. Chicago, IL, USA: American Institute of Aeronautics and Astronautics, 2009, aIAA Paper No. 2009-xxxx.

[17] K. Bilimoria, "A geometric optimization approach to aircraft conflict resolution," in *AIAA Guidance, Navigation, and Control Conference*, vol. AIAA 2000-4265, Denver, CO, August 2000.

[18] G. Dowek, C. Munoz, and V. Carremo, "Provably safe coordinated strategy for distributed conflict resolution," in *AIAA Guidance, Navigation, and Control Conference and Exhibit*, San Francisco, CA, August 2005.

[19] Federal Aviation Administration, "NextGen Annual Report - Fiscal Year 2023, *U.S. Department of Transportation*," 2023.

[20] European commission, "COMMISSION IMPLEMENTING REGULATION (EU) 2021/664 of 22 April 2021 on a regulatory framework for the U-space, european union aviation safety agency," 2021.

[21] ——, "Commission Implementing Regulation (EU) 2021/665 of 22 April 2021 amending Implementing Regulation (EU) 2017/373 as regards requirements for providers of air traffic management/air navigation services and other air traffic management network functions in the U-space airspace designated in controlled airspace, european union aviation safety agency," 2021.

[22] ——, "Commission Implementing Regulation (EU) 2021/666 of 22 April 2021 amending Regulation (EU) No 923/2012 as regards requirements for manned aviation operating in U-space airspace, european union aviation safety agency," 2021.

[23] Spanish Aviation Safety and Security Agency (AESA). (n.d.) U-space service providers (ussps). Accessed on April 28, 2025. Describes U-Space service providers and their role in drone operations. [Online]. Available: https://www.seguridadaerea.gob.es/en/ambitos/navegacion-aerea/proveedores-de-servicios-u-space

[24] European Union Aviation Safety Agency (EASA), *Easy Access Rules for U-space*, 2024, online publication.

[Online]. Available: https://www.easa.europa.eu/en/document-library/easy-access-rules/online-publications/easy-access-rules-u-space

[25] ——, "High-level regulatory framework for the u-space," Cologne, Germany, 2020. [Online]. Available: https://www.easa.europa.eu/sites/default/files/dfu/Opinion%20No%2001-2020.pdf

[26] M. Johnson, "High capacity UAM ports," NASA AEWG Presentation, 2022, accessed: 2025-04-29. [Online]. Available: https://ntrs.nasa.gov/api/citations/20220007613/downloads/20220007613_Johnson_AEWG_presentation_final_2.pptx.pdf

[27] Z. Bilgin, I. Yavrucuk, and M. Bronz, "Urban air mobility guidance with panel method: Experimental evaluation under wind disturbances," *Journal of Guidance, Control, and Dynamics*, vol. 47, pp. 1–17, 04 2024.

[28] J. Van den Berg, S. J. Guy, and D. Manocha, "Optimal reciprocal collision avoidance for multi-agent navigation," in *2010 IEEE International Conference on Robotics and Automation*. IEEE, 2010, pp. 705–711.

[29] T. Chauvin, D. Gianazza, and N. Durand, "ORCA-A* : A Hybrid Reciprocal Collision Avoidance and Route Planning Algorithm for UAS in Dense Urban Areas," in *14^{th} SESAR Innovation Days*, 2024.

[30] R. Fremond, Y. Xu, and G. Inalhan, "Adaptive Multi-Agent Reinforcement Learning Solver for Tactical Conflict Resolution in Diverse Urban Airspace Configurations," *IEEE Transactions on Aerospace and Electronic Systems, vol. 61, no. 2, pp. 2802-2820*, 2024.

[31] Z. Bilgin, M. Bronz, and I. Yavrucuk, "Experimental evaluation of robustness of panel-method-based path planning for urban air mobility," in *AIAA Aviation Forum*, 27 June-1 July 2022.

[32] ——, "Experimental evaluation of panel-method-based path planning for evtol in a scaled urban environment," in *Vertical Flight Society Forum 78*, May 10-12 2022.

[33] ——, "Panel method based guidance for fixed wing micro aerial vehicles," in *International Micro Air Vehicle Conference and Competition*, Sep 2022.

[34] J. D. Anderson, *Fundamentals of Aerodynamics*, 5th ed. McGraw-Hill, 2011.

[35] J. Katz and A. Plotkin, *Low Speed Aerodynamics*. Cambridge, UK: Cambridge Univ. Press, 2001.

[36] International Civil Aviation Organization, "Airborne Collision Avoidance System (ACAS) Manual, Doc 9863, *3^{rd} Edition*," Montreal, Quebec, Canada, 2021.

[37] American Society for Testing and Materials, "Standard Specification for Detect and Avoid System Performance Requirements, F3442/F3442M-20, vol. 15.09," 2022.

[38] RTCA Inc., *DO-386, Minimum Operational Performance Standards for Airborne Collision Avoidance System Xu (ACAS Xu), Volume I and II*, 2020.

[39] ——, *DO-396, Minimum Operational Performance Standards for Airborne Collision Avoidance System sXu (ACAS sXu), Volume I and II*, 2022.

[40] L. E. Alvarez, I. Jessen, M. P. Owen, J. Silbermann, and P. Wood, "ACAS sXu: Robust Decentralized Detect and Avoid for Small Unmanned Aircraft Systems," in *38^{th} Digital Avionics Systems Conference*, 2019.